

Causal Discovery Under a Confounder Blanket

David Watson¹ and Ricardo Silva¹

¹University College London

Corresponding author: david.watson@ucl.ac.uk

Abstract

Inferring causal relationships from observational data is rarely straightforward, but the problem is especially difficult in high dimensions. For these applications, causal discovery algorithms typically require parametric restrictions or extreme sparsity constraints. We relax these assumptions and focus on an important but more specialized problem, namely recovering a directed acyclic subgraph of variables known to be causally descended from some (possibly large) set of confounding covariates, i.e. a *confounder blanket*. This is useful in many settings, for example when studying a dynamic biomolecular subsystem with genetic data providing causally relevant background information. Under a structural assumption that, we argue, must be satisfied in practice if informative answers are to be found, our method accommodates graphs of low or high sparsity while maintaining polynomial time complexity. We derive a sound and complete algorithm for identifying causal relationships under these conditions and implement testing procedures with provable error control for linear and nonlinear systems. We demonstrate our approach on a range of simulation settings.

1 Introduction

Discovering causal relationships between variables is a vital first step in any effort to understand complex systems or design effective interventions. In principle, such relationships can be established through sufficient experimentation; in practice, we must often make do with observational data due to logistical or ethical constraints. Causal discovery algorithms designed to learn directed acyclic graphs (DAGs) have been in use for decades—see [Glymour et al., 2019] for a recent review—but the task is notoriously difficult and error-prone, especially in high-dimensional settings. Moreover, many of these methods, for computational or statistical tractability, assume *scale-free sparsity*—i.e., that for each vertex in the true unknown graph, its number of adjacencies does not grow with the dimensionality of the problem.

In many cases, researchers are interested primarily in the causal relationships between just a subset of observed variables. Attempting to learn the whole DAG in such cases is inefficient and unstable, especially when error rate control is a concern and unmeasured confounders cannot be ruled out. Suppose, however, that we have access to a large tier of background factors \mathbf{Z} that may potentially deconfound our target system \mathbf{X} . This stratification could be due to temporal ordering or physical laws. For example, we know that genotypes precede phenotypes, even though it may be impossible to completely characterize the relationship between the two, let alone links among the genotypes themselves. We argue that many practical problems of interest exhibit such a two-tier structure, with our *foreground* variables \mathbf{X} causally preceded by some large *background* set \mathbf{Z} , whose internal structure is not relevant or even well-defined.

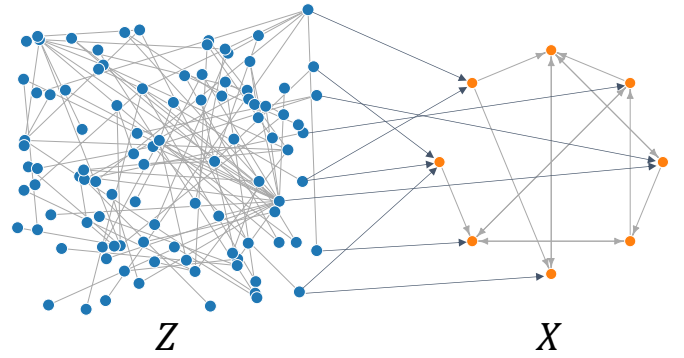


Figure 1: Visual depiction of our setup, which includes a large collection of background variables \mathbf{Z} (blue nodes) with arbitrary structure, followed by a relatively small set of foreground variables \mathbf{X} (orange nodes). The goal is to learn causal relationships among \mathbf{X} variables by exploiting signals from \mathbf{Z} .

We propose a novel solution specifically designed for downstream directed acyclic subgraph (subDAG) discovery. Our method leverages “pre-system” background covariates \mathbf{Z} to establish causal relationships among foreground variables \mathbf{X} without making any assumptions about the sparsity of connections between the two tiers. The trade-off is that it will not attempt to discover every possible structural signature that a typical causal discovery method can in theory resolve [Spirtes et al., 2000]. Instead, we limit ourselves to what can be derived from the background-foreground interaction. In particular, we posit that background variables can act as a *confounder blanket*, which, as a whole, either blocks unmeasured confounding or not. This amounts to a bet that we can avoid combinatorial search over subsets of \mathbf{Z} and still get informative results.

Our main contributions are threefold. (1) We derive a sound and complete set of rules for inferring causal order in subDAGs with background variables, as well as identifiability conditions for causal discovery in such settings. Completeness is derived with respect to a so-called *lazy oracle*, which we argue is of greater practical relevance in many settings than the classical independence oracle, especially when we are concerned about statistical and computational feasibility. (2) We design an algorithm that implements these rules with finite sample error control, making a further assumption about how to test for statistical independencies based on regression models. The method is efficient and flexible, avoiding the combinatorial search associated with alternative methods and accommodating both linear and nonlinear systems. (3) We test our approach against a range of alternatives on simulated and real-world data, confirming that the method recovers ancestral relationships in the target DAG with high power and bounded error.

2 Background and Notation

We assume that causal relationships can be encoded as a DAG \mathcal{G} . Each vertex in \mathcal{G} represents a random variable in a distribution with density/mass function $p(\cdot)$. We make use of the following common terminology in causal discovery: *parent*, *child*, *ancestor*, *descendant*, *collider*, (*active/backdoor*) *path*, *d-separation* and *Markov equivalence class*. We omit formal definitions due to space constraints. For details, see [Spirtes et al., 2000, Pearl, 2009a].

We use $\mathbf{X} \perp\!\!\!\perp_{\mathcal{G}} \mathbf{Y} \mid \mathbf{Z}$ to denote that set \mathbf{X} is *d-separated* from set \mathbf{Y} given set \mathbf{Z} in \mathcal{G} . The notation is deliberately similar to that of conditional independence in probability theory [Dawid, 1979]. We stipulate that the joint distribution of the data is Markov with respect to \mathcal{G} , i.e. $\mathbf{X} \perp\!\!\!\perp_{\mathcal{G}} \mathbf{Y} \mid \mathbf{Z} \Rightarrow \mathbf{X} \perp\!\!\!\perp \mathbf{Y} \mid \mathbf{Z}$. When the distribution is *faithful* to the graph, the converse holds as well, upgrading the relationship to a biconditional: $\mathbf{X} \perp\!\!\!\perp_{\mathcal{G}} \mathbf{Y} \mid \mathbf{Z} \Leftrightarrow \mathbf{X} \perp\!\!\!\perp \mathbf{Y} \mid \mathbf{Z}$.

Given two vertices X and Y in \mathcal{G} , we use $X \prec Y$ to denote that X is an ancestor of Y . Equivalently, $Y \succ X$ denotes that Y is a descendant of X . We write $X \preceq Y$ if X is *not a descendant* of Y , in which case X may or may not be an ancestor of Y . (Note that $X \not\prec Y$ implies $Y \preceq X$.) We write $X \sim Y$ when neither variable is an ancestor of the other, i.e. $X \not\prec Y$ and $Y \not\prec X$. Relations \prec and \preceq can be applied to pairs of sets, implying that the relation holds between each pair of elements from the Cartesian product of the respective sets.

Let $\mathbb{E}[Y \mid do(X = x)]$ denote the expected *outcome* Y under an intervention that fixes the *treatment* X to level x . *Covariate adjustment* postulates that

$$\mathbb{E}[Y \mid do(X = x)] = \int_{\mathbf{Z}} \mathbb{E}[Y \mid x, \mathbf{z}] p(\mathbf{z}) d\mathbf{z}$$

for a set of vertices $\mathbf{Z} \preceq (X, Y)$ in \mathcal{G} . It holds if \mathbf{Z} satisfies the *backdoor criterion* with respect to (X, Y) [Pearl, 2009a,

Ch. 3], in which case we say that \mathbf{Z} is a *valid adjustment set* for (X, Y) .

Finally, we define minimal (de)activators, originally highlighted by Claassen and Heskes [2011]:

Definition 1 (Minimal activator). Variable D is a *minimal activator* of the relationship between A and B given \mathbf{C} iff: (1) $A \not\perp\!\!\!\perp B \mid \mathbf{C} \cup D$; and (2) $A \perp\!\!\!\perp B \mid \mathbf{C}$. In this case, we write $A \not\perp\!\!\!\perp B \mid \mathbf{C} \cup [D]$. \square

Definition 2 (Minimal deactivator). Variable D is a *minimal deactivator* of the relationship between A and B given \mathbf{C} iff: (1) $A \perp\!\!\!\perp B \mid \mathbf{C} \cup D$; and (2) $A \not\perp\!\!\!\perp B \mid \mathbf{C}$. In this case, we write $A \perp\!\!\!\perp B \mid \mathbf{C} \cup [D]$. \square

3 Problem Statement

Assume a DAG \mathcal{G} contains *observable* vertices $\mathbf{Z} \cup \mathbf{X}$, consisting of *background* variables \mathbf{Z} and *foreground* variables \mathbf{X} . Let $|\mathbf{Z}| = d_Z$ and $|\mathbf{X}| = d_X$, with potentially $d_Z \gg d_X$. \mathcal{G} may have unobserved (hidden) vertices \mathbf{U} with more than one descendant in $\mathbf{Z} \cup \mathbf{X}$ (i.e., *unmeasured confounders*). Without loss of generality [Pearl, 2009a, Sect. 2.6], we assume that each $U \in \mathbf{U}$ has no parents and exactly two children in $\mathbf{Z} \cup \mathbf{X}$. Interchangeably, we can replace any path $X_i \leftarrow U_{ij} \rightarrow X_j$ with a *bidirected edge* $X_i \leftrightarrow X_j$ forming an *acyclic directed mixed graph* (ADMG) with vertex set $\mathbf{Z} \cup \mathbf{X}$. Its Markov properties follow from marginalizing the hidden variables of the corresponding DAG [Richardson, 2003]. The symbol $\mathcal{G}^{\mathbf{U}}$ will denote the ADMG of \mathcal{G} .

The goal is to infer as much as possible about the causal structure of $\mathcal{G}_X \subset \mathcal{G}$, which consists of vertices \mathbf{X} and the edges with endpoints in \mathbf{X} . We make the following assumptions:

- (A1) \mathcal{G} is acyclic.
- (A2) $p(\mathbf{z}, \mathbf{x})$ is faithful to $\mathcal{G}^{\mathbf{U}}$.
- (A3) \mathbf{Z} contains no descendant of \mathbf{X} in \mathcal{G} , i.e. $\mathbf{Z} \preceq \mathbf{X}$.

The first assumption can be relaxed— \mathcal{G}_Z may contain cycles under some conditions—but we adopt it here to avoid further technicalities. Faithfulness is a common yet somewhat controversial starting point for many causal discovery procedures (more on this in Sect. 7). The ordering assumption applies in many settings where background knowledge permits a categorical distinction between upstream and downstream variables, e.g. when data are recorded at different times.

For any pair of variables $X, Y \in \mathbf{X}$, exactly one of three possibilities obtains: (G1) $X \prec Y$; (G2) $X \succ Y$; or (G3) $X \sim Y$. Our discovery problem is defined as deciding which relationship holds for each pair of vertices in \mathcal{G}_X . A similar goal motivates Magliacane et al. [2016], who derive a general algorithm called ancestral causal inference (ACI). ACI does not exploit the background-foreground split and does not scale to high dimensionality. It also comes with no theory about the error control of its statistical decisions. Note that some relationships in \mathcal{G}_X may be only partially identifiable, e.g. if all we can determine is

that $X \preceq Y$. Others may be entirely unidentifiable, e.g. if latent confounding is present.

In the next section, we describe a causal discovery algorithm that assumes we have an *oracle* capable of returning exact information about which conditional independencies hold in the population. This is so that we can more easily discuss the limits of what can in principle be discovered from the assumptions provided. In Sect. 5, we present a practical statistical algorithm with error control guarantees.

4 Confounder Blankets and The Oracle Algorithm

There are sound and complete algorithms, based on the fast causal inference (FCI) algorithm of [Spirtes et al. \[2000\]](#), which return all and only graphs which are equivalent to the true \mathcal{G} in terms of implied d -separations—i.e., they are in the same *Markov equivalence class* [[Zhang, 2008](#)].¹

Such methods scale poorly with data dimensionality, as they must query for conditional independence over an exponentially increasing number of candidate conditioning sets. For tractability, sometimes it is assumed that \mathcal{G} is sparse or small [e.g. [Magliacane et al., 2016](#)], an unrealistic assumption if we think each element of \mathbf{X} should be directly connected to a substantive fraction $\mathcal{O}(d_Z)$ of background variables—a type of structure taken for granted in most methods that estimate causal effects by covariate adjustment [[Hernán and Robins, 2009](#)]. Instead, this work is based on the following principle:

Definition 3 (The Confounder Blanket Principle, CBP). In the presence of a large set of background variables \mathbf{Z} , where it is believed that each element of \mathbf{X} may be adjacent to $\mathcal{O}(d_Z)$ elements of \mathbf{Z} in \mathcal{G}^U , do not attempt to test for conditional independencies using arbitrary subsets of \mathbf{Z} . In particular, work under the expectation that if some $\mathbf{A} \subset \mathbf{Z} \cup \mathbf{X}$ is a valid adjustment set for any ordered pair $X_i \prec X_j$, then $\mathbf{A} \cup \mathbf{Z}$ is also valid. We call a set of background variables with this property a *confounder blanket*. \square

A failure of CBP does not compromise the *soundness* of the algorithms presented in the sequel, but it might affect their *informativeness*. In particular, under CBP, we are exposed to the problem of *M-structures* [[Pearl, 2009b](#)], where a path $X_i \leftarrow \dots \rightarrow Z_k \leftarrow \dots \rightarrow X_j$ is active given \mathbf{Z} , but no other paths between X_i and X_j are active given (some subset of) $\mathbf{Z} \setminus \{Z_k\}$. This means we might miss constraints that would allow us to infer $X_i \prec X_j$.

M-structures can indeed make a substantive impact to the bias of an adjustment set. However, [Ding and Miratrix \[2015\]](#) have shown that, at least at under some reasonable distributions of parameters in some parametric models,

¹In theory, their output can be refined with background knowledge, such as partial orientation, by simply excluding those members of the equivalence class that are incompatible with the given knowledge.

their impact may be negligible with high probability, and hence, statistically hard to detect in a causal discovery method. Instead of proposing yet another derivative of FCI, we believe that practitioners with access to a large set of background variables—which may be required in order to stand a chance against unmeasured confounding—are better served by methods grounded in the CBP.

4.1 Structural Signatures and Algorithm

Our algorithm will be based on the following inference rules, adapted from [Entner et al. \[2013\]](#) and [Magliacane et al. \[2016\]](#). In what follows, let \mathbf{A} and $\{X, Y\}$ be two sets of vertices in a causal graph \mathcal{G} where $\mathbf{A} \preceq \{X, Y\}$, and let $\mathbf{A}_{\setminus W} := \mathbf{A} \setminus \{W\}$ for some vertex W . Our first rule detect (indirect) causes via relations of minimal independence:

- (R1) If $\exists W \in \mathbf{A}$ such that $W \perp\!\!\!\perp Y \mid \mathbf{A}_{\setminus W} \cup \{X\}$, then $X \prec Y$.

The soundness of (R1), and (R2) below, follows immediately from Lemma 1 of [Magliacane et al. \[2016\]](#), combined with the partial order $\mathbf{A} \preceq \{X, Y\}$. (R1) applies when X *deactivates* all paths from W to Y . When this structure obtains, causal effects can be estimated using the backdoor adjustment with admissible sets \mathbf{A} and $\mathbf{A}_{\setminus W}$ [see [Pearl, 2009a](#), Ch. 3].

Our second inference rule eliminates (indirect) causes via relations of minimal dependence:

- (R2) If $\exists W \in \mathbf{A}$ such that $W \not\perp\!\!\!\perp X \mid \mathbf{A}_{\setminus W} \cup \{Y\}$, then $X \preceq Y$.

(R2) applies when Y *activates* some path from W to X . This means that Y must be a (descendant of a) collider on that path, and cannot be a non-collider on any other path active under $\mathbf{A}_{\setminus W}$.

Our third rule establishes causal independence via separating sets, and follows immediately from faithfulness:

- (R3) If $X \perp\!\!\!\perp Y \mid \mathbf{A}$, then $X \sim Y$.

These building blocks are the basis for our confounder blanket learner (CBL), outlined in Alg. 1. It outputs a square and lower triangular ancestrality matrix \mathbf{M} , with \mathbf{M}_{ij} representing the partial order between vertices (X_i, X_j) . The subscript \mathbf{M} on a partial ordering relation indicates that it is already encoded in the ancestrality matrix, which evolves with each pass through the for loop. The oracle \mathcal{I} is an indicator function over conditional independencies on $p(\mathbf{z}, \mathbf{x})$.

4.2 Properties

Proofs for all theorems are given in Appx. A.

Theorem 1 (Soundness). *All ancestral relationships returned by CBL-ORACLE hold in the true \mathcal{G}_X . Moreover, if $\mathbf{M}_{ij} = i \prec j$, then the set of non-descendants used to infer this fact, $\mathbf{A} = \mathbf{Z} \cup \{X \in \mathbf{X} \setminus \{X_i, X_j\} : X \preceq_{\mathbf{M}} \{X_i, X_j\}\}$, is a valid adjustment set for (X_i, X_j) .*

Algorithm 1 CBL-ORACLE

Input: Background set \mathbf{Z} , foreground set \mathbf{X} , oracle \mathcal{I}
Output: Ancestrality matrix \mathbf{M}

```

Initialize: converged  $\leftarrow$  FALSE,  $\mathbf{M} \leftarrow [\text{NA}]$ 
while not converged do
  converged  $\leftarrow$  TRUE
  for  $X_i, X_j \in \mathbf{X}$  such that  $i > j$ ,  $\mathbf{M}_{ij} = [\text{NA}]$  do
     $\mathcal{A} \leftarrow \mathbf{Z} \cup \{X \in \mathbf{X} \setminus \{X_i, X_j\} : X \preceq_{\mathbf{M}} \{X_i, X_j\}\}$ 
    if  $\mathcal{I}(X_i \perp\!\!\!\perp X_j \mid \mathcal{A})$  then
       $\mathbf{M}_{ij} \leftarrow i \sim j$ , converged  $\leftarrow$  FALSE
    end if
    for  $W \in \mathcal{A}$  do
      if  $\mathcal{I}(W \perp\!\!\!\perp X_j \mid \mathcal{A}_{\setminus W} \cup [X_i])$  then
         $\mathbf{M}_{ij} \leftarrow i \prec j$ , converged  $\leftarrow$  FALSE
      else if  $\mathcal{I}(W \perp\!\!\!\perp X_i \mid \mathcal{A}_{\setminus W} \cup [X_j])$  then
         $\mathbf{M}_{ij} \leftarrow j \prec i$ , converged  $\leftarrow$  FALSE
      else if  $\mathcal{I}(W \not\perp\!\!\!\perp X_j \mid \mathcal{A}_{\setminus W} \cup [X_i])$  then
         $\mathbf{M}_{ij} \leftarrow j \preceq i$ , converged  $\leftarrow$  FALSE
      else if  $\mathcal{I}(W \not\perp\!\!\!\perp X_i \mid \mathcal{A}_{\setminus W} \cup [X_j])$  then
         $\mathbf{M}_{ij} \leftarrow i \preceq j$ , converged  $\leftarrow$  FALSE
      end if
    end for
  end for
end while

```

By design, CBL-ORACLE can be uninformative where a method like FCI will provide a causal order. One of the simplest examples is the so-called *Y-structure* [Mani et al. \[2006\]](#), $\{X_1 \rightarrow X_3, X_2 \rightarrow X_3, X_3 \rightarrow X_4\}$, where FCI discovers $X_3 \rightarrow X_4$. By contrast, with an empty \mathbf{Z} , CBL-ORACLE cannot infer any causal ordering (though it may still infer $X \sim Y$ via (R3)). However, the presence of a single edge from a background variable into X_1, X_2 , or X_3 will allow for the discovery of $X_3 \prec X_4$; an edge from Z into X_4 will allow for the discovery that X_4 is not an ancestor of any other variables.

We characterize (full) identifiability conditions for CBL-ORACLE as follows, with $\mathbf{X}_{\preceq i}$ standing for the set of all X_i 's non-descendants in \mathcal{G}_X , including X_i itself.

Theorem 2 (Identifiability). *The following conditions are necessary and sufficient to find the total causal order of \mathbf{X} within ADMG \mathcal{G}^U : (i) there is no active backdoor path between any pair $\{X_i, X_j\}$ given \mathbf{Z} and their common ancestors in \mathbf{X} ; (ii) for each pair $\{X_i, X_j\}$ such that $X_i \prec X_j$ in \mathcal{G} , X_i has at least one adjacent vertex $V \in \mathbf{X}_{\preceq i}$ in \mathcal{G}^U that is not d-connected to X_j given $\mathbf{X}_{\preceq i} \setminus \{V\}$.*

Condition (i) above motivates the name *confounder blanket*.

One of the key points, however, is the *completeness* of our algorithm. In the nonparametric causal discovery literature, this is usually defined with respect to an oracle that delivers true answers to all conditional independence queries over observable variables. We define a new scope for completeness that places some reasonable limits on oracular omnipotence. First, we introduce the following definitions:

Definition 4 (Iteration- t known non-descendant). Given an algorithm \mathcal{A} , we call vertex W an *iteration- t known non-descendant* of a vertex X if (i) $W \in \mathbf{Z}$, or (ii) after t modifications to \mathbf{M} by \mathcal{A} , the algorithm has deduced that $W \preceq X$. \square

Definition 5 (Lazy oracle algorithm). Let $\mathbf{X}_{\preceq i}^t$ be the set of all iteration- t known non-descendants of X_i according to some algorithm \mathcal{A} . A *lazy oracle algorithm* is one that starts with an uninformative ancestrality matrix \mathbf{M} and updates at each round t with answers to queries of just two types:

- (i) $W \perp\!\!\!\perp X_i \mid \mathbf{S}_{ij \setminus W}^t \cup \phi(X_j)$, such that $W \in \mathbf{S}_{ij}^t$ and $\phi(X_j) \in \{\emptyset, \{X_j\}\}$; and
- (ii) $X_i \perp\!\!\!\perp X_j \mid \mathbf{S}_{ij}^t$,

where $\{X_i, X_j\} \subseteq \mathbf{X}$ and $\mathbf{S}_{ij}^t := \mathbf{X}_{\preceq i}^t \cap \mathbf{X}_{\preceq j}^t$. \square

Our oracle may be clairvoyant when it comes to probabilistic relationships, but she is not quite as accommodating as her classical counterpart. In particular, she cannot be bothered to marshal her powers in service of combinatorial search strategies, which she considers inelegant and tedious. Instead she bestows her favor upon us only when we limit ourselves to a more restrictive class of queries pertaining to independence relationships conditioned on the complete set of (known) non-descendants for any given pair of foreground variables.

Observe that inferences about ancestral relationships are fully ordered with respect to their information content: $\{\text{NA}\} \prec \{i \preceq j\} \prec \{i \prec j\} \sim \{i \sim j\}$. This motivates the following optimality target:

Definition 6 (Dominance). Among the set of all sound procedures for learning ancestral relationships, we say that algorithm \mathcal{A} *dominates* algorithm \mathcal{B} iff \mathcal{A} is strictly more informative than \mathcal{B} . That is, (i) there exists no pair of vertices in any DAG \mathcal{G} such that \mathcal{A} 's output for that pair is less informative than \mathcal{B} 's; and (ii) there exists some pair of vertices in some DAG \mathcal{G} such that \mathcal{A} 's output for that pair is more informative than \mathcal{B} 's. \square

Finally, we may state our completeness result.

Theorem 3 (Completeness). *No lazy oracle algorithm dominates CBL-ORACLE. That is, inferences returned by CBL-ORACLE are always at least as informative as those of any lazy oracle algorithm.*

Of course, relationships of conditional independence are estimated from finite samples in practice. In the sequel, we consider practical methods for implementing an algorithm that is pointwise consistent under further assumptions about the nature of conditional independencies in $p(\mathbf{z}, \mathbf{x})$.

5 Statistical Inference

In this section, we describe a practical method based on the oracle algorithm, called CBL-SAMPLE. Our main

assumption to help bridge the gap between theory and practice is the following:

- (A4) We have access to a regression algorithm by which we can test any pairwise conditional independence statement $X \perp\!\!\!\perp Y \mid \mathbf{S}$ by regressing Y on $\mathbf{S} \cup \{X\}$. The regression is implemented with a variable selection strategy which will, in the limit of infinite data, remove X from the regression equation if and only if $X \perp\!\!\!\perp Y \mid \mathbf{S}$.

Statistical error control techniques are presented under this assumption. We will not discuss its validity for the specific sparse regression engines exploited here. This is well-understood in, for example, the case of Gaussian linear regression and a z -test of the coefficient for X . In other scenarios, due to computational or statistical reasons, this is less straightforward (e.g., lasso is “sparsistent” only under restrictive assumptions, and it is possible to have a covariate dropping out of a population regression function even if the corresponding conditional independence does not hold [Hastie et al., 2015]). Instead, we take this foundational assumption as an idealization that simplifies analysis, being open about the fact that, in practice, such assumptions may only be approximately satisfied.

Constraints like $W \perp\!\!\!\perp X_j \mid \mathbf{A}_{\setminus W} \cup [X_i]$ suggest two regression models per triplet (X_i, X_j, W) : one for the regression of X_j on W , $\mathbf{A}_{\setminus W}$ and X_i , and another for the regression of X_j on W and $\mathbf{A}_{\setminus W}$ only. In the algorithm that follows, we simplify this by using a single model to simultaneously test for all W , fitting a regression for X_j on \mathbf{A} and X_i , and another regression for X_j on \mathbf{A} only. These are clearly mathematically equivalent (as $\mathbf{A} = \mathbf{A}_{\setminus W} \cup \{W\}$), so long as the variable selection procedure in the regression model can be computed exactly, for instance when using z -tests for a Gaussian regression model or when lasso sparsistency conditions are satisfied. This will not necessarily be the case when an intractable combinatorial search underlies variable selection, or when conditions for a continuous relaxation do not hold. The safer alternative is, just like in the oracle algorithm, to perform individualized model selection for each W , without any concern for simultaneously selecting variables within $\mathbf{A}_{\setminus W}$.

Nevertheless, for simplicity we rely on a joint variable selection procedure that uses all elements of \mathbf{A} when fitting each regression model, and empirically show that bundling individual covariate tests achieves better results than existing alternatives. We emphasize that combinatorial search can be avoided altogether by separating selection on each W from any sort of sparse regularization or search among the other covariates, if so desired.

Bipartite Subgraphs. We begin with the simplest case, in which we have just two foreground variables $\mathbf{X} = \{X, Y\}$. We fit a quartet of models to estimate the following conditional expectations:

$$\begin{aligned} f_Y^0 &: \mathbb{E}[Y \mid \mathbf{Z}] & f_X^0 &: \mathbb{E}[X \mid \mathbf{Z}] \\ f_Y^1 &: \mathbb{E}[Y \mid \mathbf{Z}, X] & f_X^1 &: \mathbb{E}[X \mid \mathbf{Z}, Y], \end{aligned}$$

where subscripts index outcome variables and superscripts differentiate between full and reduced conditioning sets. Assume, for concreteness, that all structural equations are linear. Since some elements of \mathbf{Z} may not influence \mathbf{X} , we could estimate the members of this quartet using lasso regression, which performs automatic feature selection. This results in four different *active sets* of predictors. For instance, the active set $\hat{S}_Y^0(\lambda) \subseteq \mathbf{Z}$ picks out just those background variables that receive nonzero weight in the model \hat{f}_Y^0 at a given value of the regularization parameter λ (though we generally suppress the dependence for notational convenience).

Our basic strategy is to refit the model quartet some large number of times B , taking different training/validation splits to get a sampling distribution over active sets. (The exact resampling method is described in more detail below.) This allows us to test the antecedent of (R3) by evaluating whether $X \in \hat{S}_Y^1$ or $Y \in \hat{S}_X^1$ with sufficient frequency. If either event occurs fewer than γB times (with the convention that $\gamma = 1/2$) we conclude that $X \sim Y$. Because we seek to minimize errors of commission, we are more conservative in our inference procedures for \prec and \preceq relations. From our distribution of active sets we calculate the (de)activation rate of each non-descendant with respect to a given causal ordering. This gives four unique rates per non-descendant, representing the (de)activation frequencies when treating either X or Y as the candidate cause. High rates are evidence that the corresponding inference rule applies.

What is a reasonable threshold for drawing such an inference? It is not immediately obvious how to specify an expected null (de)activation rate without further assumptions on the data generating process. Rather than introduce some ad-hoc prior or sparsity constraint, we take an adaptive approach inspired by the stability selection procedure of Meinshausen and Bühlmann [2010]. Specifically, we use a variant of complementary pairs stability selection [Shah and Samworth, 2013], which guarantees an upper bound on the probability of falsely selecting a low-rate feature at any given threshold τ . The method is so named because, on each draw b , we partition the data into disjoint sets of equal size. Rates are estimated over all $2B$ subsamples.

Stability selection was originally conceived for controlling error rates in feature selection problems, primarily lasso regression. We adapt the procedure to accommodate our modified target, which is a conjunction of inclusion/exclusion statements rather than a single selection event. Specifically, we are interested in the probability of (de)activation under some fixed feature selection procedure \hat{S} . We write:

$$r_d(Z_k)_{X \preceq Y} := \mathbb{P}(Z_k \in \hat{S}_Y^0 \wedge Z_k \notin \hat{S}_Y^1)$$

to denote the probability that feature Z_k is deactivated w.r.t. $X \preceq Y$. Activation rates are analogously defined:

$$r_a(Z_k)_{X \preceq Y} := \mathbb{P}(Z_k \notin \hat{S}_X^0 \wedge Z_k \in \hat{S}_X^1).$$

For the opposite ordering, we simply swap active sets, using \hat{S}_X^0, \hat{S}_X^1 for deactivation, and \hat{S}_Y^0, \hat{S}_Y^1 for activation w.r.t. $X \succeq Y$.

Definition 7 (Complementary pairs stability selection). Let $\{(\mathcal{D}_{2b-1}, \mathcal{D}_{2b}) \subseteq [n] : b \in [B]\}$ be randomly chosen independent pairs of sample subsets of size $\lfloor n/2 \rfloor$ such that $\mathcal{D}_{2b-1} \cap \mathcal{D}_{2b} = \{\emptyset\}$. For $\tau \in [0, 1]$, $\phi \in \{a, d\}$, and $\psi \in \{X \preceq Y, X \succeq Y\}$, the complementary pairs stability selection (CPSS) procedure is $\hat{\mathbf{H}}_{\tau, \phi, \psi} := \{k : \hat{r}_\phi(Z_k)_\psi \geq \tau\}$, with estimated rates given by:

$$\hat{r}_d(Z_k)_{X \preceq Y} := \#\{b : Z_k \in \hat{S}_Y^0(\mathcal{D}_b) \wedge Z_k \notin \hat{S}_Y^1(\mathcal{D}_b)\}/2B$$

for deactivation w.r.t. $X \preceq Y$, and

$$\hat{r}_a(Z_k)_{X \preceq Y} := \#\{b : Z_k \notin \hat{S}_X^0(\mathcal{D}_b) \wedge Z_k \in \hat{S}_X^1(\mathcal{D}_b)\}/2B$$

for activation w.r.t. the same ordering. Again, to estimate rates for the opposite ordering, we simply swap active sets as described above. \square

For some $\theta < \tau$, let $\mathbf{L}_{\theta, \phi, \psi} := \{k : r_\phi(Z_k)_\psi \leq \theta\}$ denote the set of low-rate variable indices for some ϕ, ψ . Our goal is to bound the expected number of low-rate features selected at a given threshold τ , i.e. $\mathbb{E}[|\hat{\mathbf{H}}_{\tau, \phi, \psi} \cap \mathbf{L}_{\theta, \phi, \psi}|]$. Methods for doing so rely on certain assumptions about the distribution of rates for features within $\mathbf{L}_{\theta, \phi, \psi}$. [Shah and Samworth \[2013\]](#)’s tightest bound is achieved under r -concavity, which is formally defined in Appx. B. Roughly, r -concave distributions describe a continuum of constraints that interpolate between unimodality and log-concavity for $r \in [-\infty, 0]$. Simulation results suggest that (de)activation rates for low-rate features exhibit the following property (see Appx. B):

(A5) For all $Z \in \mathbf{L}_{\theta, \phi, \psi}$, empirical rates $\hat{r}_\phi(Z)_\psi$ are approximately $-1/4$ -concave.

We now have the following error control guarantee:

Theorem 4 (Error control). *The expected number of low-rate features selected by the CPSS procedure is bounded from above:*

$$\mathbb{E}[|\hat{\mathbf{H}}_{\tau, \phi, \psi} \cap \mathbf{L}_{\theta, \phi, \psi}|] \leq \min\{D(\theta^2, 2\tau - 1, B, -1/2), D(\theta, \tau, 2B, -1/4)|\mathbf{L}_{\theta, \phi, \psi}|\},$$

where $D(\theta, \tau, B, r)$ is the maximum of $\mathbb{P}(X \geq \tau)$ over all r -concave random variables supported on $\{0, 1/2B, 1/B, \dots, 1\}$ with $\mathbb{E}[X] \leq \theta$.

This is a direct application of [Shah and Samworth \[2013\]](#)’s Eq. 8. Though the bound is valid for all $\tau \in (\theta, 1]$, we apply an adaptive lower bound $\epsilon > \theta$, which denotes the minimum rate such that no conflicting inferences emerge, e.g. different ancestors deactivating for opposite causal orderings. We follow the authors’ recommendations for default values of B and θ (see Appx. B). We note that there is no closed form solution for $D(\theta, \tau, B, r)$, but the quantity is easily computed with numerical methods. If the number of (de)activations detected via this procedure exceeds the maximum error bound of Thm. 4, we infer that at least one must be a true positive. Since even a single (de)activation is sufficient to partially order variable pairs, this licenses the corresponding inference.

General case. Our method can be expanded to accommodate larger sets of foreground variables and nonlinear structural equations. When $d_X > 2$, we simply loop through all $d_X(d_X - 1)/2$ unique pairs of variables and record any inferences made at time $t = 1$. Like in the oracle algorithm, as the set \mathbf{A} grows for $t > 1$, we continue cycling through pairs that have yet to be unambiguously decided until no further inferences are forthcoming. Though we use lasso regression for linear systems in our experiments, stepwise regression or even best subset selection may be viable alternatives [[Hastie et al., 2020](#)]. For nonlinear systems, we use gradient boosted regression trees with early stopping, which automatically adapt to signal sparsity [[Friedman, 2001](#), [Bühlmann and Yu, 2003](#)]. Any function $s : \mathbb{R}^d \times \mathbb{R} \mapsto 2^d$ from input variables and outcome to an active set of predictors will suffice. All we require of our feature selection subroutine s is that it be a consistent estimator for the Markov blanket of a given variable, a criterion that is satisfied under fairly minimal conditions [see, e.g., [Candès et al., 2018](#), Prop. 1].

In the worst case, CBL-SAMPLE requires $\mathcal{O}(Bd_X^3)$ operations per feature selection subroutine s , the complexity of which itself presumably depends on n, d_Z and d_X . For example, with $n > d = (d_Z + d_X)$, the least angle regression implementation of lasso takes $\mathcal{O}(d^3 + nd^2)$ computations [[Efron et al., 2004](#)], resulting in overall complexity of $\mathcal{O}(B(d_X^6 + nd_X^5 + d_Z^3))$. More generally, if s executes in polynomial time, then CBL-SAMPLE is of complexity order P . Since constraint-based graphical learning without sparsity restrictions is NP-hard [[Chickering et al., 2004](#)], this represents a major computational improvement. The procedure can be sped up even further by parallelizing over subsamples, as these are independent. For pseudocode summarizing CBL-SAMPLE, see Alg. 3 in Appx. C.

6 Experiments

Full details of our simulation experiments are described in Appx. D. Briefly, we vary the sample size and dimensionality of the data, as well as graph structure and sparsity. Linear and nonlinear structural equations are applied at a range of different signal-to-noise ratios (SNRs).

6.1 Bipartite Subgraphs

We benchmark against a constraint-based method proposed by [Entner et al. \[2013\]](#) and a score-based alternative similar in spirit to many causal discovery algorithms. We highlight two key differences between our proposal and the constraint-based alternative: (1) [Entner et al. \[2013\]](#)’s method assumes a partial order on foreground variables upfront. With the prior knowledge that $X \preceq Y$, it tests whether $X \rightarrow Y$ or $X \sim Y$, with the possibility that the disjunction is undecidable from the observational distribution. It therefore has an advantage in the following experiment, where the partial ordering assumption is satisfied, but competitors still consider the possibility that $X \leftarrow Y$. (2) The original version of [Entner et al. \[2013\]](#)’s method performs combinatorial search through the space

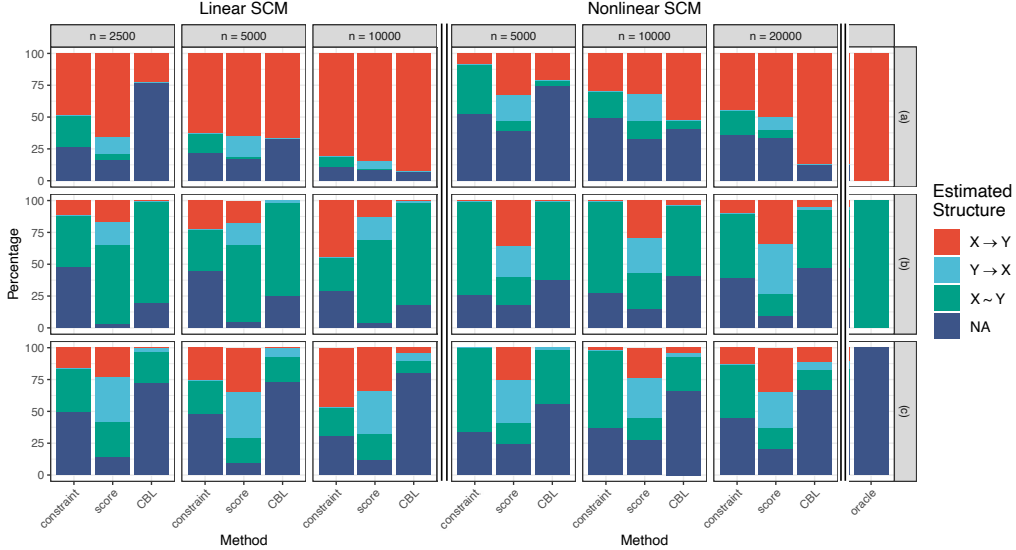


Figure 2: Simulation results at varying sample sizes for three different structures: (a) $X \rightarrow Y$; (b) $X \perp\!\!\!\perp_{\mathcal{G}} Y \mid \mathbf{S}$; and (c) $X \perp\!\!\!\perp_{\mathcal{G}} Y \mid \mathbf{S} \cup [\mathbf{U}]$. We compare our CBL method to constraint- and score-based benchmarks. Expected results of an independence oracle are included at the far right.

of non-descendants, which is infeasible in our setting. Following the authors’ advice, we simplify the procedure by sampling random variable-subset pairs from \mathbf{Z} , evaluating conditional independence either via partial correlation (for linear data) or the generalized covariance measure [Shah and Peters, 2020] with gradient boosting subroutine (for nonlinear data).

For our score-based benchmark, we train a series of models to evaluate three different structural hypotheses, corresponding to (G1) $X \rightarrow Y$; (G2) $X \leftarrow Y$; and (G3) $X \sim Y$. We use lasso for linear data and gradient boosting for nonlinear data. We calculate the proportion of variance explained on a test set for all settings. If (G3) scores highest, we return $X \sim Y$. Otherwise, we test whether out-of-sample residuals for the top scoring model are correlated with the foreground predictor. If so, we return NA; if not, we return whichever of (G1) or (G2) scored highest.

We visualize results for the setting with 100 background variables and expected sparsity $1/2$ (see Fig. 2). Data are simulated from 100 random graphs drawn under three different structural constraints: (a) $X \rightarrow Y$; (b) $X \perp\!\!\!\perp_{\mathcal{G}} Y \mid \mathbf{S}$, for some $\mathbf{S} \subseteq \mathbf{Z}$; and (c) $X \perp\!\!\!\perp_{\mathcal{G}} Y \mid \mathbf{S} \cup [\mathbf{U}]$, where \mathbf{U} denotes a set of latent confounders. The first two are identifiable, while the third is not. Linear and nonlinear structural equations are applied with $\text{SNR} = 2$.

We find that CBL fares well in all settings. Constraint-based methods show less power to detect edges when present in this experiment, especially in nonlinear systems, while score-based methods incur higher error rates when edges are absent. We also observe that the constraint-based procedure requires considerable tuning—we had to experiment with a five-dimensional grid of decision thresholds to get reasonable results—and is by far the slowest to execute, taking about five times longer than

CBL even with the random subset approach.

6.2 Larger Subgraphs

We benchmark against two popular causal discovery algorithms: really fast causal inference (RFCI), a constraint-based method proposed by Colombo et al. [2012] as a more scalable version of the original FCI algorithm [Spirtes et al., 2000]; and greedy equivalence search (GES), a score-based alternative due to Meek [1997] and Chickering [2003]. Both algorithms can be computed with background information to encode our partial ordering assumption, and restricted to focus on the subgraph \mathcal{G}_X . Despite its name, RFCI struggles to converge in reasonable time (< 24 hours) when $n = 1000$ and d_Z is on the order of 100, so we limit comparisons here to smaller datasets and run fewer replications for this method (5) than we do for GES (20). This illustrates how the assumption of extreme sparsity is necessary for RFCI to work in practice.

For this simulation, we draw random graphs of varying sample size with low (0.25) and high (0.75) sparsity, $d_Z \in \{50, 100\}$, and $d_X = 6$. Relationships are linear throughout, with RFCI using partial correlation tests for conditional independence and GES scoring edges according to BIC. Accuracy is measured with respect to all pairwise relationships for which a decision is reached. We find that CBL is more accurate on average in nearly all settings, with especially strong results in the high-sparsity, high-dimensionality regime. However, our method can be less stable than GES, as illustrated by the greater variance of results, particularly in dense networks where CBL outputs a relatively large number of NAs.

6.3 Causal Effects

Since our method identifies admissible sets for all detected edges, we may estimate the average treatment effect

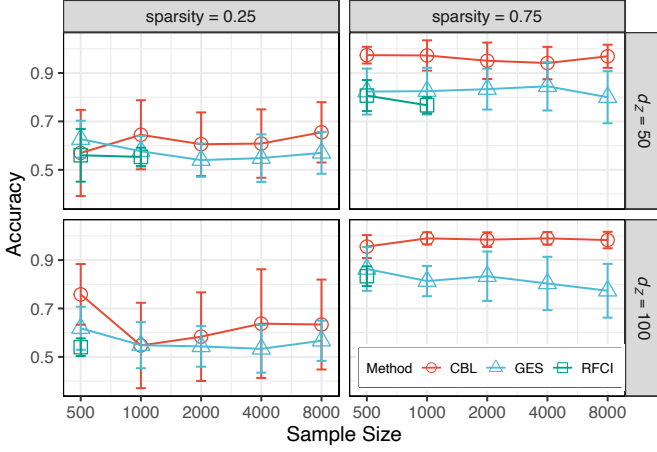


Figure 3: Simulation results for our multivariate experiment, benchmarking against RFCI and GES. Whiskers represent standard errors.

(ATE) via backdoor adjustment. For this experiment, we simulate data from a partially linear model as originally parametrized by [Robinson \[1988\]](#):

$$\begin{aligned} X &= f(\mathbf{Z}) + \epsilon_X, & \mathbb{E}[\epsilon_X | \mathbf{Z}] &= 0, \\ Y &= \beta X + g(\mathbf{Z}) + \epsilon_Y, & \mathbb{E}[\epsilon_Y | \mathbf{Z}, X] &= 0, \end{aligned}$$

with $X \in \{0, 1\}$ and $Y \in \mathbb{R}$. The goal is to estimate β , which corresponds to the ATE. We run our pipeline with three different estimators: double machine learning (DML) [[Chernozhukov et al., 2018](#)], inverse propensity weighting (IPW) [[Rosenbaum and Rubin, 1983](#)], and targeted maximum likelihood estimation (TMLE) [[van der Laan and Rose, 2011](#)]. For all three methods, models are fit with gradient boosting and parameters estimated via cross-fitting to avoid regularization bias. We simulate 1000 datasets with $\beta = 1, d_Z = 100, n = 10000$, and $\text{SNR} \in \{1/2, 1, 2\}$. We find that all three methods provide consistent ATE estimates, with TMLE generally performing best in terms of bias and variance (see Fig. 4). This illustrates how CBL can be combined with existing algorithms to go beyond causal discovery and into causal inference.

7 Discussion

We have proposed a novel method for learning ancestral relationships in downstream subgraphs based on the confounder blanket principle, which advises against combinatorial search for conditioning sets in cases where scale-free sparsity cannot be safely assumed. Our CBL algorithm is provably sound and complete with respect to a lazy oracle. Our sample version controls errors of commission with high probability and compares favorably to constraint- and score-based alternatives in a range of trials. In addition to accurately learning ancestral relationships, CBL identifies valid adjustment sets for causal effect estimation.

We note several limitations of our method. First, CBL will struggle in the presence of weak edges. For instance, if the true graph is $\mathbf{Z} \rightarrow X \rightarrow Y$ and $I(X; Y) \gg I(X; \mathbf{Z})$, then conditioning on Y in finite samples could deactivate some path(s) from \mathbf{Z} to X , leading to the erroneous inference

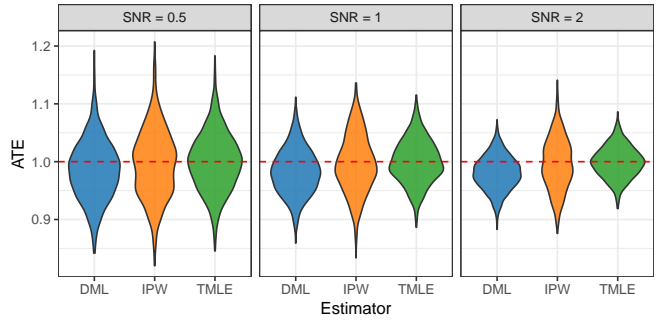


Figure 4: Average treatment effects estimated by combining CBL with three different algorithms at varying SNRs.

$Y \rightarrow X$. We observe that weak edges pose problems for all causal discovery procedures. Indeed, one motivation for taking an inclusive approach to background variables is the hope that a sufficiently large confounder blanket should include at least some strong edges that can be exploited to learn structural information about \mathcal{G}_X .

CBL relies on the assumption of faithfulness, which has been challenged by numerous authors [[Cartwright, 2001](#), [Steel, 2006](#), [Zhang and Spirtes, 2008](#), [Andersen, 2013](#), [Uhler et al., 2013](#)]. Several weaker variants have been proposed, including SGS-minimality [[Spirtes et al., 2000](#)], P-minimality [[Pearl, 2009a](#)], frugality [[Forster et al., 2018](#)], and 2-adjacency faithfulness [[Marx et al., 2021](#)]. One direction for future work is to extend CBL under these relaxed assumptions.

The current implementation of CBL is order-dependent, inasmuch as estimated subgraphs for the same dataset may vary if columns are reordered. This can be addressed using methods previously devised for constraint-based causal discovery [[Colombo and Maathuis, 2014](#)].

ACKNOWLEDGMENTS. This work was supported by ONR grant 62909-19-1-2096. We thank Joshua Loftus for helpful comments on an earlier draft of this manuscript.

References

- Holly Andersen. When to expect violations of causal faithfulness and why it matters. *Phil. Sci.*, 80(5):672–683, 2013.
- Peter Bühlmann and Bin Yu. Boosting with the L_2 loss. *J. Am. Stat. Assoc.*, 98(462):324–339, 2003.
- Emmanuel Candès, Yingying Fan, Lucas Janson, and Jinchi Lv. Panning for gold: ‘model-X’ knockoffs for high dimensional controlled variable selection. *J. R. Statist. Soc. B*, 80(3):551–577, 2018.
- Nancy Cartwright. What is wrong with Bayes nets? *Monist*, 84(2):242–264, 2001.
- Victor Chernozhukov, Denis Chetverikov, Mert Demirer, Esther Duflo, Christian Hansen, Whitney Newey, and James Robins. Double/debiased machine learning for

- treatment and structural parameters. *Econom. J.*, 21(1):C1–C68, 2018.
- David Maxwell Chickering. Optimal structure identification with greedy search. *J. Mach. Learn. Res.*, 3: 507–554, 2003.
- David Maxwell Chickering, David Heckerman, and Christopher Meek. Large-sample learning of Bayesian networks is NP-hard. *J. Mach. Learn. Res.*, 5:1287–1330, 2004.
- Tom Claassen and Tom Heskes. A logical characterization of constraint-based causal discovery. In *Proceedings of the 27th Conference on Uncertainty in Artificial Intelligence*, pages 135–144, 2011.
- Diego Colombo and Marloes H. Maathuis. Order-independent constraint-based causal structure learning. *J. Mach. Learn. Res.*, 15(116):3921–3962, 2014.
- Diego Colombo, Marloes H. Maathuis, Markus Kalisch, and Thomas S. Richardson. Learning high-dimensional directed acyclic graphs with latent and selection variables. *Ann. Statist.*, 40(1):294 – 321, 2012.
- A P Dawid. Conditional independence in statistical theory. *J. R. Statist. Soc. B*, 41(1):1–31, 1979.
- Peng Ding and Luke Miratrix. To adjust or not to adjust? Sensitivity analysis of M-bias and butterfly-bias. *J. Causal Inference*, 3(1):41–57, 2015.
- Bradley Efron, Trevor Hastie, Iain Johnstone, and Robert Tibshirani. Least angle regression. *Ann. Stat.*, 32(2): 407 – 499, 2004.
- Doris Entner, Patrik Hoyer, and Peter Spirtes. Data-driven covariate selection for nonparametric estimation of causal effects. In *Proceedings of the 16th International Conference on Artificial Intelligence and Statistics*, pages 256–264, 2013.
- Malcolm Forster, Garvesh Raskutti, Reuben Stern, and Naftali Weinberger. The frugal inference of causal relations. *Br. J. Philos. Sci.*, 69(3):821–848, 2018.
- Jerome H. Friedman. Greedy function approximation: A gradient boosting machine. *Ann. Statist.*, 29(5):1189 – 1232, 2001.
- Jerome H. Friedman, Trevor Hastie, and Rob Tibshirani. Regularization paths for generalized linear models via coordinate descent. *J. Stat. Softw.*, 33(1):1–22, 2010.
- Clark Glymour, Kun Zhang, and Peter Spirtes. Review of causal discovery methods based on graphical models. *Front. Genet.*, 10:524, 2019.
- Trevor Hastie, Robert Tibshirani, and Martin Wainwright. *Statistical learning with sparsity: The lasso and generalizations*. Chapman & Hall/CRC, Boca Raton, FL, 2015.
- Trevor Hastie, Robert Tibshirani, and Ryan Tibshirani. Best subset, forward stepwise or lasso? Analysis and recommendations based on extensive comparisons. *Statist. Sci.*, 35(4):579–592, 2020.
- Miguel A Hernán and James M Robins. *Causal Inference: What If*. Chapman & Hall/CRC, Boca Raton, 2009.
- Markus Kalisch, Martin Mächler, Diego Colombo, Marloes H. Maathuis, and Peter Bühlmann. Causal inference using graphical models with the R package pcalg. *J. Stat. Softw.*, 47(11):1–26, 2012.
- Guolin Ke, Qi Meng, Thomas Finley, Taifeng Wang, Wei Chen, Weidong Ma, Qiwei Ye, and Tie-Yan Liu. Lightgbm: A highly efficient gradient boosting decision tree. In *Advances in Neural Information Processing Systems*, volume 30, 2017.
- Sara Magliacane, Tom Claassen, and Joris M. Mooij. Ancestral causal inference. In *Advances in Neural Information Processing Systems 30*, page 4473–4481, 2016.
- Subramani Mani, Peter Spirtes, and Gregory Cooper. A theoretical study of Y structures for causal discovery. In *Proceedings of the 22nd Conference on Uncertainty in Artificial Intelligence*, pages 314–323, 2006.
- Alexander Marx, Arthur Gretton, and Joris M. Mooij. A weaker faithfulness assumption based on triple interactions. In *Proceedings of the 37th Conference on Uncertainty in Artificial Intelligence*, pages 451–460, 2021.
- Christopher Meek. *Graphical Models: Selecting Causal and Statistical Models*. PhD thesis, Carnegie Mellon University, 1997.
- Nicolai Meinshausen and Peter Bühlmann. Stability selection. *J. R. Statist. Soc. B*, 72(4):417–473, 2010.
- Judea Pearl. *Causality: Models, Reasoning, and Inference*. Cambridge University Press, New York, 2nd edition, 2009a.
- Judea Pearl. Myth, confusion, and science in causal analysis. *UCAL Cognitive Systems Lab, Technical Report TR-348*, 2009b.
- Thomas Richardson. Markov properties for acyclic directed mixed graphs. *Scand. J. Stat.*, 30(1):145–157, 2003.
- P. M. Robinson. Root-n-consistent semiparametric regression. *Econometrica*, 56(4):931–954, 1988.
- Paul R. Rosenbaum and Donald B. Rubin. The central role of the propensity score in observational studies for causal effects. *Biometrika*, 70(1):41–55, 1983.
- Rajen D. Shah and Jonas Peters. The hardness of conditional independence testing and the generalised covariance measure. *Ann. Statist.*, 48(3):1514 – 1538, 2020.
- Rajen D. Shah and Richard J. Samworth. Variable selection with error control: Another look at stability selection. *J. R. Statist. Soc. B*, 75(1):55–80, 2013.
- Peter Spirtes, Clark N. Glymour, and Richard Scheines. *Causation, Prediction, and Search*. The MIT Press, Cambridge, MA, 2nd edition, 2000.

- Daniel Steel. Homogeneity, selection, and the faithfulness condition. *Minds Mach.*, 16(3):303–317, 2006.
- Caroline Uhler, Garvesh Raskutti, Peter Buhlmann, and Bin Yu. Geometry of the faithfulness assumption in causal inference. *Ann. Statist.*, 41(2):436–463, 2013.
- Mark J. van der Laan and Sherri Rose. *Targeted learning: Causal Inference for Observational and Experimental Data*. Springer, New York, 2011.
- Jiji Zhang. On the completeness of orientation rules for causal discovery in the presence of latent confounders and selection bias. *Artif. Intell.*, 172(16):1873–1896, 2008.
- Jiji Zhang and Peter Spirtes. Detection of unfaithfulness and robust causal inference. *Minds Mach.*, 18(2): 239–271, 2008.

A Proofs

A.1 Proof of Theorem 1

CBL-ORACLE exhaustively applies (R1), (R2), and (R3) only to non-descendants that were confirmed to be such either by assumption (\mathbf{Z}) or by previous application of the rules. Therefore, it boils down to the soundness of the rules themselves, as the starting set of non-descendants for all $X \in \mathbf{X}$ is \mathbf{Z} . As we mentioned in the main text, (R3) is a direct application of faithfulness since the conditioning set contains no descendants of X or Y . The correctness of (R1) and (R2) are a direct application of Lemma 1 of Magliacane et al. [2016] and the partial order knowledge.

In order to obtain $\mathbf{M}_{ij} = i \prec j$, it must be the case that (R1) was used with some $\mathbf{A} = \mathbf{Z} \cup \{X \in \mathbf{X} \setminus \{X_i, X_j\} : X \preceq \{X_i, X_j\}\}$ to detect a minimal deactivation of the form $W \perp\!\!\!\perp X_j \mid \mathbf{A}_{\setminus W} \cup [X_i]$ for some $W \in \mathbf{A}$. Since this confirms that $X_i \prec X_j$, we satisfy the assumptions of Entner et al. [2013]’s (R1). Therefore, using the same arguments, we conclude that both \mathbf{A} and $\mathbf{A}_{\setminus W}$ are valid adjustment sets for (X_i, X_j) . \square

A.2 Proof of Theorem 2

Without loss of generality, for any d_X , assume that set X_1, X_2, \dots, X_{d_X} is indexed so that no X_i is a descendant of some X_j for $j > i$.

Let us start with $d_X = 2$. By hypothesis, X_1 has a vertex Z that is adjacent to it but not to X_2 . Moreover, there is no active backdoor path between Z and X_2 given $\mathbf{Z} \setminus \{Z\}$. It is also the case that $\mathbf{Z} \setminus \{Z\}$ will block all backdoor paths between X_1 and X_2 . To see this, imagine any path between X_1 and X_2 , given $\mathbf{Z} \setminus \{Z\}$, starting with (X_1, Z) as the initial edge. If Z is a collider on this path, it will be inactive. But even if Z is not a collider, the rest of this path is not active by hypothesis. Therefore, if the edge $X_1 \rightarrow X_2$ exists, (R1) will activate and we will learn the relation $X_1 \prec X_2$. If the edge does not exist, (R3) will activate and we will learn the relation $X_1 \sim X_2$.

Now, assume we are able to solve all ancestral relations for \mathcal{G}_X . As X_1 and X_{d_X} satisfy the premises with ancestral set \mathbf{Z} , we will learn either $X_1 \prec X_{d_X}$ or $X_1 \sim X_{d_X}$. Hence, we will know all the common ancestors of X_2 and X_{d_X} which are in \mathbf{X} . We also know that conditioning on all of these ancestors will not create an active backdoor path between X_2 and X_{d_X} , since we know that \mathbf{Z} is a valid adjustment set for (X_1, X_2) and either \mathbf{Z} or $\mathbf{Z} \cup \{X_1\}$ is a valid adjustment set for (X_2, X_3) . We can redefine a new \mathbf{Z} by adding X_1 to it, and iterate the argument. \square

A.3 Proof of Theorem 3

Given that CBL-ORACLE performs all possible tests allowed for a lazy oracle algorithm (subject to the conditions of finding all possible non-descendants at each iteration), this boils down to guaranteeing we are not failing to take into account further implications of (R1)-(R3) and that the non-ancestral relationships are built up properly as iterations progress.

Let’s start with the case $d_X = 2$, and then prove the general case by induction. The case $d_X = 2$ is similar to Entner et al. [2013], except we do not assume a causal order between X_1 and X_2 . This implies, for instance, that we cannot distinguish $Z \rightarrow X_1 \leftarrow X_2$ from $Z \rightarrow X_1 \leftrightarrow X_2$, unlike the algorithm of Entner et al. [2013].

When $d_X = 2$, we can refer to (R1)-(R3) with $\mathbf{A} = \mathbf{Z}$ and, without loss of generality, $X = X_1$ and $Y = X_2$. There is at most one possible modification that can be made to \mathbf{M} , so we only need to consider \mathbf{Z} as the set of non-descendants of $\{X_1, X_2\}$. If some lazy oracle algorithm \mathcal{A} dominates CBL-ORACLE, then there exists some DAG \mathcal{G}' that is indistinguishable from \mathcal{G} according to (R1)-(R3), but for which \mathcal{A} draws a more informative inference. Assume, for concreteness, that CBL-ORACLE outputs $X_1 \preceq X_2$ but \mathcal{A} outputs $X_1 \prec X_2$.

The completeness of our (R1) follows from the completeness of (R1) in Entner et al. [2013]. That proof makes no use of the presumed ancestrality relationship between X_1 and X_2 , except that their algorithm does not need to flip the roles of X_1 and X_2 when applying the rules. We do the flip, but as shown before, the algorithm remains sound.

Assume (R3) cannot be applied \mathcal{G} . It is clear that it cannot be applied to \mathcal{G}' either, since adding an edge to \mathcal{G} (that is, $X_1 \rightarrow X_2$) cannot introduce further independencies.

Assume (R1) cannot be applied to \mathcal{G} . Now, given $X_1 \not\perp_{\mathcal{G}} X_2 \mid \mathbf{Z}$ (that is, (R3) does not apply to \mathcal{G}), there is at least one path $\mathcal{P} := X_1 \leftarrow \dots \rightarrow X_2$ which is active given \mathbf{Z} in \mathcal{G} . We will show that no $W \in \mathbf{Z}$ exists such that $W \perp_{\mathcal{G}'} X_2 \mid \mathbf{Z}_{\setminus W} \cup [X_1]$, i.e., (R1) does not apply to \mathcal{G}' either. To see this, assume that (R1) does apply to \mathcal{G}' . Then, $W \perp_{\mathcal{G}'} X_2 \mid \mathbf{Z}_{\setminus W} \cup \{X_1\}$, which implies $W \perp_{\mathcal{G}} X_2 \mid \mathbf{Z}_{\setminus W} \cup \{X_1\}$, since adding edge $X_1 \rightarrow X_2$ cannot create any new independence. It is not possible that $W \not\perp_{\mathcal{G}} X_2 \mid \mathbf{Z}_{\setminus W}$, otherwise (R1) would fire and incorrectly imply that $X_1 \rightarrow X_2$ in \mathcal{G} . Hence, $W \perp_{\mathcal{G}} X_2 \mid \mathbf{Z}_{\setminus W}$. Given that $X_1 \perp_{\mathcal{G}} X_2 \mid \mathbf{Z}_{\setminus W} \cup \{W\}$ by hypothesis, W cannot be in \mathcal{P} . Since $X_1 \rightarrow X_2$ is not in the equivalent \mathcal{P} path in \mathcal{G}' , W must be connected to X_1 via some other path \mathcal{P}' into X_1 that is active given $\mathbf{Z}_{\setminus W}$ in order for X_1 to d -separate X_2 from W . But the concatenation of \mathcal{P}' with \mathcal{P} in \mathcal{G}' will

contradict $W \perp\!\!\!\perp_{\mathcal{G}'} X_2 \mid \mathbf{Z}_{\setminus W} \cup \{X_1\}$. By symmetry with the case where $X_2 \rightarrow X_1$ is added, (R1) cannot be applied to either \mathcal{G} nor \mathcal{G}' .

Assume (R2) cannot be applied to \mathcal{G} . Now, assume there exists some $W \in \mathbf{Z}$ such that $W \not\perp\!\!\!\perp_{\mathcal{G}'} X_2 \mid \mathbf{Z}_{\setminus W} \cup \{X_1\}$, i.e., (R2) applies to \mathcal{G}' . This will also imply $W \perp\!\!\!\perp_{\mathcal{G}} X_2 \mid \mathbf{Z}_{\setminus W}$, as adding the edge could not have created a new independence. Therefore, it must be the case that $W \perp\!\!\!\perp_{\mathcal{G}} X_2 \mid \mathbf{Z}_{\setminus W} \cup \{X_1\}$, otherwise (R2) would fire for \mathcal{G} . This again results in a path \mathcal{P}' which, concatenated with $X_1 \rightarrow X_2$, will contradict $W \perp\!\!\!\perp_{\mathcal{G}'} X_2 \mid \mathbf{Z}_{\setminus W}$.

Hence, for $d_X = 2$, any failure to infer a structural relationship present in \mathcal{G} using (R1)-(R3) also means that there exists some different graph, with the same answers to the oracle, where that structural feature is not present.

Assume this is the case for all \mathcal{G} with $d_X = n$, for some $n > 2$. We will show this is also the case for $d_X = n + 1$.

Let X_d be any foreground vertex in \mathcal{G} that has no children. The graph implied by the removal of X_d , $\mathcal{G}_{\setminus d}$, will have all of its lazy oracle identifiable pairwise ancestral relationships in \mathbf{M} resolved by the induction hypothesis and the fact that no descendants of a pair $\{X_i, X_j\}$ can be used in the conditioning set of an oracle query. Assuming there exists some t by which we will find all possible non-descendants of $X_i \in \mathbf{X} \setminus X_d$ (which is the case for the exhaustive search done by CBL-ORACLE), the oracle can then be invoked to sort all pairwise ancestral relationships involving X_d for iterations greater than t . \square

A.4 Proof of Theorem 4

As noted in the text, this is simply an instance of [Shah and Samworth \[2013\]](#)'s Eq. 8, adapted for our modified target, which is a conjunction of inclusion and exclusion statements rather than a single selection event. The arguments from their proof go through just the same so long as empirical rates $\hat{r}_\phi(Z)_\psi$ for all $Z \in \mathbf{L}_{\theta, \phi, \psi}$ are $-1/4$ -concave distributed. See Appendix B for empirical evidence supporting this assumption.

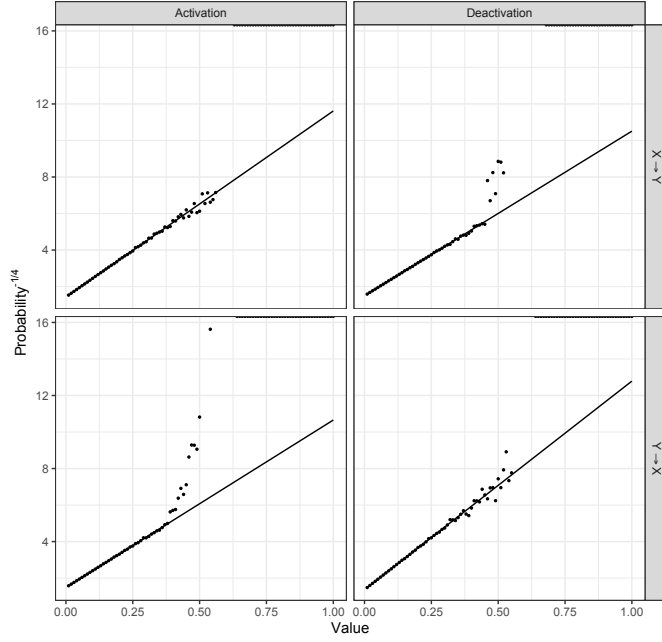


Figure 5: Example probability mass functions of $\hat{r}_\phi(Z_k)_\psi$, $Z_k \in \mathbf{L}_{\theta, \phi, \psi}$ (black points), alongside the $-1/4$ -concave distribution (smooth line), which has maximum tail probability beyond 0.4. Differences in expected values are due to variation in θ across rates. See [Shah and Samworth, 2013, Appx. A.4].

B Stability Selection

The following definition of r -concavity is from Shah and Samworth [2013, Sect. 3.3]. To define the r -concave distribution, recall that the r^{th} generalized mean $M_r(a, b; \lambda)$ of $a, b \geq 0$ is given by

$$M_r(a, b; \lambda) = \{(1 - \lambda)a^r + \lambda b^r\}^{1/r}$$

for $r > 0$. This is also well-defined for $r < 0$ if we take $M_r(a, b; \lambda) = 0$ when $ab = 0$, and define $0^r = \infty$. In addition, we may define

$$\begin{aligned} M_0(a, b; \lambda) &:= \lim_{r \rightarrow 0} M_r(a, b; \lambda) = a^{1-\lambda} b^\lambda \\ M_{-\infty}(a, b; \lambda) &:= \lim_{r \rightarrow -\infty} M_r(a, b; \lambda) = \min(a, b). \end{aligned}$$

We may now define r -concavity.

Definition 8. A non-negative function f on an interval $I \subset \mathbb{R}$ is r -concave if, for every $x, y \in I$ and $\lambda \in (0, 1)$, we have:

$$f((1 - \lambda)x + \lambda y) \geq M_r(f(x), f(y); \lambda).$$

Definition 9. A probability mass function f supported on $\{0, 1/B, 2/B, \dots, 1\}$ is r -concave if the linear interpolant to $\{(i, f(i/B)) : i = 0, 1, \dots, B\}$ is r -concave.

We find that the empirical probability mass functions of (de)activation rates for low-rate features are approximately $-1/4$ -concave. The fit is tightest for the lowest rates, which occur with the greatest frequency. See Fig. 5, especially the bottom left quadrants of all four panels, which account for the vast majority of probability mass. Missing observed probabilities (typically at x-axis values above 0.6) correspond to zero-frequency events, e.g. no feature is deactivated in 80% of training/validation splits.

Following the recommendations of Shah and Samworth [2013, Sect. 3.4], we use $B = 50$ complementary pairs and fix $\theta = d^{-1} \sum_{k=1}^d \hat{r}_\phi(Z_k)_\psi$ for each $\phi \in \{d, a\}$, $\psi \in \{i \preceq j, j \preceq i\}$. See Alg. 2.

Algorithm 2 STABILITYSELECTION

Input: Rates $R_{\phi,\psi}$, lower bound ϵ , number of complementary subsamples B

Output: One of $\{i \prec j, i \preceq j, j \prec i, j \preceq i, \text{NA}\}$

Initialize: $\text{pos} \leftarrow \{0_b\}_{b=1}^{2B}$, $\text{out} \leftarrow \text{NA}$

$d_R \leftarrow |R_{\phi,\psi}|$

$\hat{\theta} \leftarrow d_R^{-1} \sum_k^{d_R} \hat{r}_\phi(A_k)_\psi$

$\hat{L}_{\hat{\theta},\phi,\psi} \leftarrow \{k : \hat{r}_\phi(A_k)_\psi \leq \hat{\theta}\}$

for $\tau \in \{1/2B, 1/B, \dots, 1\}$ s.t. $\tau > \epsilon$ **do**

$\text{hi}_\tau \leftarrow \min\{D(\hat{\theta}^2, 2\tau - 1, B, -1/2), D(\hat{\theta}, \tau, 2B, -1/4)\} |\hat{L}_{\hat{\theta},\phi,\psi}|$

$\hat{H}_{\tau,\phi,\psi} \leftarrow \{k : \hat{r}_\phi(A_k)_\psi \geq \tau\}$

if $|\hat{H}_{\tau,\phi,\psi}| > \text{hi}_\tau$ **then**

$\text{pos}_b \leftarrow 1$

end if

end for

if $\sum_{b=1}^{2B} \text{pos}_b > 0$ **then**

if $\phi = d \wedge \psi = i \preceq j$ **then**

$\text{out} \leftarrow i \prec j$

else if $\phi = a \wedge \psi = i \preceq j$ **then**

$\text{out} \leftarrow i \preceq j$

else if $\phi = d \wedge \psi = j \preceq i$ **then**

$\text{out} \leftarrow j \prec i$

else if $\phi = a \wedge \psi = j \preceq i$ **then**

$\text{out} \leftarrow j \preceq i$

end if

end if

return out

C Sample Algorithm

The sample version of our CBL-ORACLE algorithm is provided in pseudocode below. The SAMPLE function draws uniformly without replacement from its first argument, producing a set of size equal to its second argument. The feature selection method s is a function with three arguments: a matrix of predictors, a vector of responses, and a set of row indices on which to operate. The output is an active set of features, as determined by the chosen method (e.g., lasso or stepwise regression).

Algorithm 3 CBL-SAMPLE

Input: Background variables \mathbf{Z} , foreground variables \mathbf{X} , feature selection method s , number of complementary subsamples B , omission threshold γ

Output: Ancestrality matrix \mathbf{M}

```

Initialize: converged  $\leftarrow$  FALSE,  $\mathbf{M} \leftarrow [\text{NA}]$ 
while not converged do
  converged  $\leftarrow$  TRUE
  for  $X_i, X_j \in \mathbf{X}$  such that  $i > j$ ,  $\mathbf{M}_{ij} = \text{NA}$  do
     $\mathbf{A} \leftarrow \mathbf{Z} \cup \{X \in \mathbf{X} \setminus \{X_i, X_j\} : X \preceq_{\mathbf{M}} \{X_i, X_j\}\}$ 
    for  $b \in [B]$  do
       $\mathcal{D}_{2b-1} \leftarrow \text{SAMPLE}([n], \lfloor n/2 \rfloor)$ 
       $\mathcal{D}_{2b} \leftarrow [n] \setminus \mathcal{D}_{2b-1}$ 
    end for
    for  $b \in [2B]$  do
       $\hat{\mathbf{S}}_i^0(\mathcal{D}_b) \leftarrow s(\mathbf{A}, X_i, \mathcal{D}_b)$ ,  $\hat{\mathbf{S}}_i^1(\mathcal{D}_b) \leftarrow s(\mathbf{A} \cup X_j, X_i, \mathcal{D}_b)$ 
       $\hat{\mathbf{S}}_j^0(\mathcal{D}_b) \leftarrow s(\mathbf{A}, X_j, \mathcal{D}_b)$ ,  $\hat{\mathbf{S}}_j^1(\mathcal{D}_b) \leftarrow s(\mathbf{A} \cup X_i, X_j, \mathcal{D}_b)$ 
    end for
     $r_i^0 \leftarrow \#\{b : X_i \notin \hat{\mathbf{S}}_j^1(\mathcal{D}_b)\} / 2B$ 
     $r_j^0 \leftarrow \#\{b : X_j \notin \hat{\mathbf{S}}_i^1(\mathcal{D}_b)\} / 2B$ 
    if  $r_i^0 > \gamma \vee r_j^0 > \gamma$  then
       $\mathbf{M}_{ij} \leftarrow i \sim j$ , converged  $\leftarrow$  FALSE
    else
      for  $A \in \mathbf{A}$  do
         $r_d(A)_{i \preceq j} \leftarrow \#\{b : A \in \hat{\mathbf{S}}_j^0(\mathcal{D}_b) \wedge A \notin \hat{\mathbf{S}}_j^1(\mathcal{D}_b)\} / 2B$ 
         $r_a(A)_{i \preceq j} \leftarrow \#\{b : A \notin \hat{\mathbf{S}}_i^0(\mathcal{D}_b) \wedge A \in \hat{\mathbf{S}}_i^1(\mathcal{D}_b)\} / 2B$ 
         $r_d(A)_{j \preceq i} \leftarrow \#\{b : A \in \hat{\mathbf{S}}_i^0(\mathcal{D}_b) \wedge A \notin \hat{\mathbf{S}}_i^1(\mathcal{D}_b)\} / 2B$ 
         $r_a(A)_{j \preceq i} \leftarrow \#\{b : A \notin \hat{\mathbf{S}}_j^0(\mathcal{D}_b) \wedge A \in \hat{\mathbf{S}}_j^1(\mathcal{D}_b)\} / 2B$ 
      end for
       $\epsilon \leftarrow \max_{\tau} \min\{\sum_{\phi \in \{d, a\}} \#\{k : r_{\phi}(A_k)_{i \preceq j} \geq \tau\}, \sum_{\phi \in \{d, a\}} \#\{k : r_{\phi}(A_k)_{j \preceq i} \geq \tau\}\} = 0$ 
      for  $\phi \in \{d, a\}, \psi \in \{i \preceq j, j \preceq i\}$  do
         $R_{\phi, \psi} \leftarrow \{A \in \mathbf{A} : r_{\phi}(A)_{\psi}\}$ 
         $\mathbf{M}_{ij} \leftarrow \text{STABILITYSELECTION}(R_{\phi, \psi}, \epsilon, B)$ 
        if  $\mathbf{M}_{ij} \neq \text{NA}$  then
          converged  $\leftarrow$  FALSE
        end if
      end for
    end if
  end for
end while

```

D Experiments

Complete code for all experiments can be found at https://github.com/dswatson/many_ancestors. Our simulation design is as follows:

- Background variables \mathbf{Z} are drawn from a multivariate normal distribution $\mathcal{N}(\mathbf{0}, \Sigma)$, where $\mathbf{0}$ denotes a length- d_Z vector of 0's and Σ is a Toeplitz matrix with autocorrelation $\rho = 0.25$. Variance for all Z 's is fixed at $1/d_Z$.
- In nonlinear settings, we create a new matrix $\tilde{\mathbf{Z}}$ in which 80% of background variables undergo some nonlinear transformation. Specifically, the following transformations are applied with equal probability:
 - **Quadratic**: $\tilde{Z} = Z^2$
 - **Square root**: $\tilde{Z} = \sqrt{|Z|}$
 - **Softplus**: $\tilde{Z} = \log(1 + \exp(Z))$
 - **ReLU**: $\tilde{Z} = \max(0, Z)$
- Edges from \mathbf{Z} to \mathbf{X} are randomly generated with some fixed probability. In the linear case, foreground variables are given by a linear combination of parents, $X_i = \sum_{j < i} \beta_{ij} A_j + \epsilon_i$, where $A_j \in \mathbf{A} = \mathbf{Z} \cup \mathbf{X}_{\prec i}$. In the nonlinear case, we substitute \tilde{A} for A , with transformations described above. Nonzero weights $\beta \neq 0$ are Rademacher distributed, i.e. drawn uniformly from $\{-1, 1\}$. Residuals ϵ_i are independent Gaussians with variance selected to ensure the target SNR.

For our bivariate experiments, we draw 100 random graphs according to each data generating process (with expected sparsity $1/2$ and $\text{SNR} = 2$) and record results with lasso regression (for linear systems) and gradient boosting (for nonlinear systems). The data generating process for the unidentifiable setting (c) is identical to (b)'s, except that half the shared parents of X and Y are removed from \mathbf{Z} .

CBL begins by splitting the data into training and test sets, with the conventional ratio 4:1. For both lasso and GBM, features are selected according to model performance on the test set. For the former, this requires a sequence of values for the regularization parameter λ , automatically generated by the `glmnet` package [Friedman et al., 2010]. For the latter, we train a forest of up to 3500 trees with early stopping if performance does not improve after 10 rounds. This is efficiently implemented via the `lightgbm` package [Ke et al., 2017]. Features never selected for splits are automatically discarded, which is how GBMs naturally accommodate sparse model fits [Bühlmann and Yu, 2003].

To implement Entner et al. [2013]'s constraint-based benchmark, we follow the authors' advice in using conditional independence tests to infer both conditional *dependence* (for low p -values) and *independence* (for high p -values). We set decision thresholds of $p < 0.1$ and $p > 0.5$ for these respective tasks. We sample 1000 variable-subset pairs for linear data and 500 for nonlinear, as the testing subroutine in the latter case is more computationally intensive. Since instances of $W \perp\!\!\!\perp Y \mid \mathbf{A}_{\setminus W} \cup [X]$ proved far more elusive than instances of $X \perp\!\!\!\perp Y \mid \mathbf{A}$ —i.e., the method finds separating sets with much higher frequency than it does minimal deactivators—we used different thresholds for these two cases. Specifically, we declare $X \rightarrow Y$ if minimal deactivations are detected in just 0.5% of all trials, while we infer $X \sim Y$ if separating sets are found in 20% of trials. These parameters were established after considerable experimentation, as the authors provide little guidance on such matters. Different data generating processes will likely require different thresholds to guarantee reasonable results.

For the score-based benchmark, we fit our model quartet with either lasso (for linear data) or GBM (for nonlinear data) and compute the proportion of variance explained on a test set of m samples via the formula

$$\text{PVE} = 1 - \frac{\sum_{i=1}^m \epsilon_i^2}{\sum_{i=1}^m (y_i - \bar{y})^2},$$

where ϵ_i denotes the model residual for sample i and Y is the outcome variable with empirical mean \bar{y} . Then, using the same indexing as above, we score the hypotheses as follows:

$$X \rightarrow Y : \hat{g}_1 = (\text{PVE}_X^0 + \text{PVE}_Y^1)/2$$

$$X \leftarrow Y : \hat{g}_2 = (\text{PVE}_Y^0 + \text{PVE}_X^1)/2$$

$$X \sim Y : \hat{g}_3 = (\text{PVE}_X^0 + \text{PVE}_Y^0)/2.$$

We evaluate potential dependencies between residuals and predictors via Pearson correlation with $\alpha = 0.1$.

Multivariate experiments were run using the RFCI and GES implementations distributed with the `pcalg` package [Kalisch et al., 2012].